RSC Advances

This article can be cited before page numbers have been issued, to do this please use: T. Wu, D. Feng, B. Xie and X. ma, *RSC Adv.*, 2016, DOI: 10.1039/C6RA01051B.

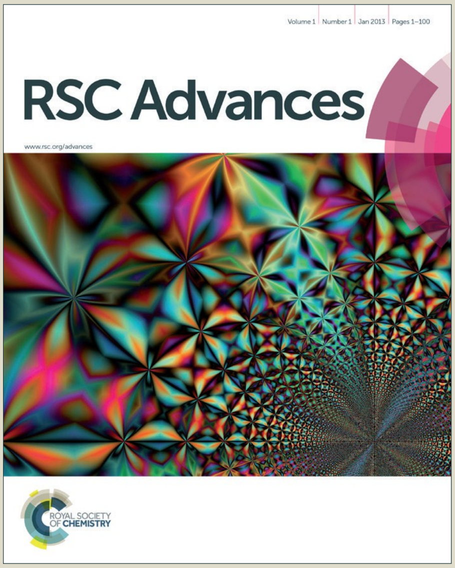

ROYAL SOCIETY OF CHEMISTRY

www.rsc.org/advances

DOI: 10.1039/C6RA01051B

Journal Name

ARTICLE

A solution to achieve good reusability of MNPs Fe_3O_4-supported (S)-Diphenylprolinoltrimethylsilyl ether catalysts in asymmetric Michael reaction

Received 00th January 20xx,
Accepted 00th January 20xx

DOI: 10.1039/x0xx00000x

www.rsc.org/

Tao Wu,[a] Dandan Feng,[a] Bing Xie*[b] and Xuebing Ma*[a]

A new supported (S)-diphenylprolinol trimethylsilyl ether (Fe_3O_4/PVP@ProTMS) using polyvinylpyrrolidone (PVP)-modified MNPs Fe_3O_4 as a support was prepared *via* one-pot surface-modification, and exhibited the high yield (93-99%), excellent diastereoselectivities (*syn/anti* = 81–96:19 – 4) and enantioselectivities (95– 98% *ee*) in the asymmetric Michael addition of propanal to various nitroalkenes. TGA, XRD, IR, SEM, TEM, elemental analysis and N_2 adsorption-desorption isotherm demonstrated that the adsorption of PVP onto MNPs Fe_3O_4 resulted in the spectacular change in the chemical composition, surface morphology and pore structure of Fe_3O_4/PVP@SiO_2/ProTMS. The catalyst could be easily separated from the reaction by an external magnet and reused for ten times with the high yields (77–99%) and unchanged excellent steroselectivities (97–98% ee and *syn/anti* = 96/4) in the Michael addition for the first time.

Introduction

The Jørgensen–Hayashi organocatalysts, i.e., *α, α*-diarylprolinoltrimethylsilyl ethers,[1] which activate aldehyde *via* an enamine [2] and *α, β*-unsaturated carbonyl compound *via* an iminium ion,[3] can be considered as one of the most famous leading actors among the versatile organocatalysts in the asymmetric reactions such as Aldol, Michael, cycloaddition, epoxidation and desymmetrization.[4] Moreover, Jørgensen–Hayashi catalysts had been utilized in asymmetric tandem and multi-component reactions, through which large quantities of enantiopure compounds with multiple stereogenic carbon centers can be conveniently constructed.[5] However, the usage of organocatalyst, typically 10–30 mol%, was needed to achieve desirable catalytic performance in most cases of organocatalyzed reactions. From the viewpoint of green chemistry, several efficient and economical protocols using polymer,[6] inorganic material,[7] ionic liquid [8] and graphene oxide [9] as catalyst supports were developed to achieve the reuse of expensive Jørgensen–Hayashi catalysts.

On the other hand, due to the potential advantages of inexpensive, non-toxic, chemically stable properties and re-collection by simple magnetic decantation without filtration or centrifugation, the magnetic nanoparticles (MNPs) of Fe_3O_4 had emerged recently as a new type of catalyst support in heterogeneous asymmetric organocatalysis with good catalytic performances, especially in Aldol addition.[10] However, in the asymmetric Michael addition of aldehyde to nitroalkene, all the reported MNPs Fe_3O_4-supported Jørgensen–Hayashi catalysts gave the unsatisfactory reusability. In 2010, W. Wang *et al*. developed Fe_3O_4@SiO_2-supported Jørgensen–Hayashi catalyst, whose yield and stereoselectivity significantly decreased to 54%, *syn/anti* = 83: 17 and 85% ee in the third run.[11] One year later, A. Pericás *et al*. immobilized Jørgensen–Hayashi catalyst onto azide functionalized MNPs Fe_3O_4@SiO_2. Unfortunately, the similar sharp drop in catalytic performance was found in the fourth run (57%, *syn/anti* = 72:28 and 92% ee).[12] Recently, A. Ouali *et al.* also reported on a poly(benzylazide)styrene-functionalized magnetic Co/C-supported (*S*)-*α, α*-diphenylprolinoltrimethylsilyl ether with a sharp drop in the activity in the 3rd run.[13] Untill now, the good reusability of MNPs-supported Jørgensen–Hayashi catalyst could not be achieved in the asymmetric Michael addition of aldehyde to nitroalkene.

In our attempts to solve the reusability of MNPs-supported Jϕrgensen-Hayashi catalyst, we report the supporting of (*S*) -*α, α*-diphenylprolinoltrimethylsilyl ether onto polyvinylpyrrolidone (PVP)-modified MNPs of Fe_3O_4 through the hydrolysis of –$Si(OCH_3)_3$ by the facile one-pot surface-modification (Scheme 1). Due to the vital function of PVP, the as-synthesized Fe_3O_4/PVP@ProTMS possessed the excellent catalytic performances (93–99% yield, *syn/anti* = 81–96:19–4, 95–98 %ee) and good reusability with the unchanged excellent steroselectivities (*syn/anti* = 96:4, 98% ee) and moderate yield (82%), even in the 10th run.

---

[a] *Key Laboratory of Applied Chemistry of Chongqing Municipality, School of Chemistry and Chemical Engineering, Southwest University, Chongqing, 400715, P. R. China. E-mail: zcj123@swu.edu.cn; Fax: +86 2368253237; Tel: +86 23 68253237.*
[b] *School of Chemistry and environmental science, Guizhou Minzhu University, Guiyang, 550025, P. R. China. E-mail: bing_xie1963@hotmail.com;. Fax: (+86)851-3610278; Tel: (+86)851-3610278.*

Electronic Supplementary Information (ESI) available: TGA, TEM and N_2 adsorption-desorption isotherm of catalysts, ^{1}H, ^{13}C NMR and HPLC spectra of intermediates and products. See DOI: 10.1039/x0xx00000x

View Article Online
DOI: 10.1039/C6RA01051B

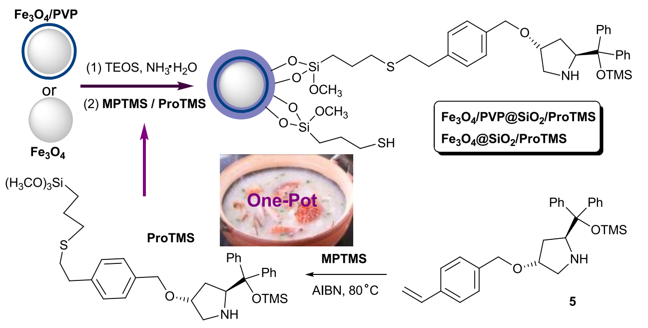

Scheme 1 The one-pot preparation of PVP-modified MNPs Fe$_3$O$_4$-supported Jørgensen–Hayashi organocatalysts

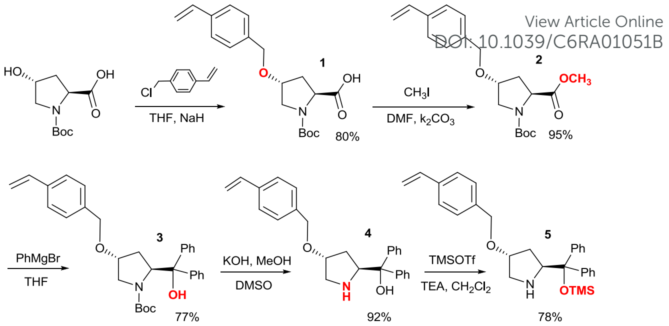

Scheme 2. The synthetic route to the Jørgensen–Hayashi organocatalyst **5**.

Experimental

Characterization

^{1}H and ^{13}C NMR spectra were conducted using a Bruker av-600 NMR instruments, in which all chemical shifts were reported down-field in ppm relative to the hydrogen and carbon resonances of TMS. FT-IR spectroscopy was performed on a Perkin-Elmer model GX spectrometer using the KBr pellet. Thermogravimetry-differential thermal analysis was carried out on a SBTQ600 thermal analyzer at a heating rate of 10 ℃ min^{-1} from 40 to 800 ℃ using N$_2$ as protective gas (100 mL min^{-1}). Elemental analysis was performed using a vario Micro cube elemental analyzer instrument. The surface morphologies of the samples were observed by JSM-6510LV scanning electron microscopy and Tecnai G2 F20 transmission electron microscope, operated at 20 Kv/15mA and 200 kV respectively. X-ray powder diffraction patterns were detected on an XRD-7000 S/L instrument: Cu-Kα radiation, X-ray tube settings of 40 kV/30 mA and a step size of 2 °min^{-1} in the 10–100 °(2*θ*) range. N$_2$ adsorption–desorption isotherm was carried out at 77.4 K using an Autosorb-1 apparatus (Quantachrome), in which the sample was degassed at 120 ℃ for 12 h before measurement, and the specific surface area and the pore diameter were calculated by the BET method and BJH model, respectively. Magnetization curve was determined by HH-15 vibrating sample magnetometer. The *syn/anti* ratios and % ee values of products were determined by ^{1}H NMR and Agilent LC-1200 HPLC using Daicel Chiralpak OD-H 4.6 mm × 25 cm column under 20 ℃, 220 nm and 1.0 mL min^{-1} conditions, respectively.

Synthesis of Jørgensen–Hayashi catalyst 5

Synthesis of compound 1: To a anhydrous THF (20 mL) suspension of NaH (0.75 g, 18.8 mmol) was added in turn 30 mL of THF solution containing Boc-L-hydroxyproline (2.0 g, 8.7 mmol), 18-crown-6 (0.23 g, 0.86 mmol) and 4-vinylbenzyl chloride (90 %, 3.66 g, 21.6 mmol) at room temperature. The reaction mixture was warmed to 50 ℃ for 12 h. The resulting mixture was added water (30 mL), extracted with cyclohexane (50 mL × 2) to remove residual 4-vinylbenzyl chloride, adjusted to pH in the range of 2–3 by saturated aqueous KHSO$_4$ solution and extracted with ethyl acetate (50 mL × 3). The combined organic layers were dried over anhydrous Na$_2$SO$_4$ and concentrated under reduced pressure. The residue was purified by silica gel gradient column chromatography using petroleum ether/ethyl acetate (*v/v* = 4/1 to 1/2) as eluents to afford yellow oil **1** (2.5 g, 80%). ^{1}H NMR (600 MHz, CDCl$_3$, TMS) *δ* 1.42–1.47 (m, 9H, C*H$_3$*), 2.10–2.46 (m, 2H, NCHC*H$_2$*), 3.51–3.73 (m, 2H, NC*H$_2$*), 4.17–4.17 (m, 1H, NC*H*), 4.36–4.53 (m, 3H, OC*H*, OC*H$_2$*), 5.24 (d, *J* = 10.8 Hz, 1H, =C*H$_2$*), 5.74 (d, *J* = 17.6 Hz, 1H, =C*H$_2$*), 6.70 (dd, *J* = 10.9, 17.6 Hz, 1H, =C*H*), 7.26–7.39 (m, 4H, Ar-*H*), 8.90 (s, 1H, COOH) ppm; ^{13}C NMR (151 MHz, CDCl$_3$): δ 28.2 (*C*H$_3$), 36.7 (NCH*C*H$_2$), 52.0 (N*C*H$_2$), 57.9 (N*C*H), 71.0, 75.9, 80.7 (O*C*H$_2$, O*C*H and O*C*(CH$_3$)$_3$), 114.0 (=*C*H$_2$), 126.3, 127.7, 127.8, 136.4, 137.2 (Ph, =*C*H), 153.9 (N*C*=O), 178.2 (*C*=O) ppm.

Synthesis of compound 2: The reaction mixture of 1 (1.0 g, 2.88 mmol) and K$_2$CO$_3$ (1.59 g, 11.53 mmol) in 10 mL of DMF was added CH$_3$I (0.49 g, 3.47 mmol) and stirred at room temperature for 1 h. Subsequently, after being quenched by water (50 mL), the resulting mixture was extracted with ethyl acetate (50 mL × 3). The combined organic layers were washed with water (50 mL × 4), dried over anhydrous Na$_2$SO$_4$ and concentrated under reduced pressure to afford the yellow oil **2** (0.99 g, 95%). ^{1}H NMR (600 MHz, CDCl$_3$, TMS) δ 1.42–1.47 (m, 9H, C*H$_3$*), 2.10–2.46 (m, 2H, NCHC*H$_2$*), 3.51–3.73 (m, 2H, NC*H$_2$*), 4.17–4.17 (m, 1H, NC*H*), 4.36–4.53 (m, 3H, OC*H*, OC*H$_2$*), 5.24 (d, *J* = 10.8 Hz, 1H, =C*H$_2$*), 5.74 (d, *J* = 17.6 Hz, 1H, =C*H$_2$*), 6.70 (dd, *J* = 10.9, 17.6 Hz, 1H, =C*H*), 7.26–7.39 (m, 4H, Ar-*H*), 8.90 (s, 1H, COOH) ppm; ^{13}C NMR (151 MHz, CDCl$_3$): δ 28.2 (CH$_3$), 36.7 (NCH*C*H$_2$), 51.3 (N*C*H$_2$), 57.9 (N*C*H), 71.0, 75.9, 80.7 (O*C*H$_2$, O*C*H and O*C*(CH$_3$)$_3$), 114.0 (=*C*H$_2$), 126.3, 127.7, 127.8, 136.4, 137.2 (Ph, =*C*H), 153.9 (N*C*=O), 178.2 (*C*=O) ppm.

Synthesis of compound 3: A N$_2$-filled three-necked flask was charged with magnesium chips (1.08 g, 45.0 mmol), bromobenzene (4.71 g，30.0 mmol) and anhydrous THF (45 mL), refluxed for 3 h and cooled to room temperature. To the obtained reaction mixture was added anhydrous THF solution containing **2** (30 mL, 3.0 g, 8.3 mmol) dropwise at 0 ℃ and stirred at room temperature for 3 h. After being quenched with aqueous NH$_4$Cl solution (50 mL), the reaction mixture was extracted with diethyl ether (100 mL × 3). The combined organic phases were dried over anhydrous Na$_2$SO$_4$ and concentrated to afford the residue, which was purified by silica gel column chromatography using petroleum ether/ethyl acetate (*v/v* = 50/1 to 20/1, 10/1 and 1/1) as eluents to afford the white powder **3** (0.75 g, 77%); ^{1}H NMR

View Article Online
DOI: 10.1039/C6RA01061B

(600 MHz, $CDCl_3$, TMS) δ 1.38 (s, 9H, CH_3), 2.08–2.18 (m, 2H, $NCHCH_2$), 2.86 (s, 1H, NC*H*), 3.35–3.52 (m, 2H, NCH_2), 4.28–4.34 (m, 2H, OCH_2), 5.02–5.05 (m, 1H, OC*H*), 5.22 (d, *J* = 10.9 Hz, 1H, $=CH_2$), 5.72 (d, *J* = 17.6 Hz, 1H, $=CH_2$), 6.69 (dd, *J* = 10.9, 17.6 Hz, 1H, =C*H*), 7.16–7.49 (m, 14H, Ar-*H*) ppm; ^{13}C NMR (151 MHz, $CDCl_3$): δ 28.2 (CH_3), 36.5 ($NCHCH_2$), 52.9 (NCH_2), 65.1 (N*C*H), 70.6, 76.4, 80.7 (OCH_2, O*C*H, O*C*$(CH_3)_3$), 81.6 (*C*OH), 113.8 ($=CH_2$), 126.2, 127.1, 127.2, 127.5, 127.8, 127.9, 136.6, 137.1, 137.5 (Ph, =*C*H), 145.7 (N*C*=O) ppm.

Synthesis of compound 4: The reaction mixture of **3** (1.47 g, 3.04 mmol) and KOH (1.68 g, 0.03 mol) in the mixed MeOH/DMSO (20 mL, *v/v* = 2/7) was stirred at 60 ℃ for 6 h, added water (20 mL) and extracted with cyclohexane (20 mL × 5). The combined organic layer was dried over anhydrous Na_2SO_4 and concentrated under reduced pressure to afford white solid **4** (1.08 g, 92%). ^1H NMR (600 MHz, $CDCl_3$, TMS) δ1.64–1.68 (m, 1H, $NCHCH_2$), 1.76–1.83 (m, 1H, $NCHCH_2$), 3.09 (s, 2H, NCH_2), 4.01–4.02 (m, 1H, NC*H*), 4.38–4.50 (m, 2H, OCH_2), 4.57 (dd, *J* = 9.6, 6.7 Hz, 1H, OC*H*), 5.23 (d, *J* = 10.9 Hz, 1H, $=CH_2$), 5.73 (d, *J* = 17.6 Hz, 1H, $=CH_2$), 6.70 (dd, *J* = 10.9, 17.6 Hz, 1H, =C*H*), 7.13–7.57 (m, 14H, Ar-*H*) ppm; ^{13}C NMR (151 MHz, $CDCl_3$): δ 33.0 ($NCHCH_2$), 52.4 (NCH_2), 63.4 (N*C*H), 70.5, 76.9, 79.5 (OCH_2, O*C*H and O*C*$(CH_3)_3$), 113.8 ($=CH_2$), 125.4, 126.0, 126.3, 126.4, 126.6, 127.8, 128.0, 128.3, 136.5, 137.1, 137.9, 144.9, 147.3 (Ph, =*C*H) ppm.

Synthesis of compound 5: Triethylamine (0.19 g, 1.9 mmol) and trimethylsilyl trifluoromethanesulfonate (TMSOTf, 0.42 g, 1.9 mmol) were added in turn at 0 ℃ to anhydrous CH_2Cl_2 solution containing **4** (15 mL, 0.39 g, 1.0 mmol) under a N_2 atmosphere. After being stirred at room temperature for 3 h, the resulting mixture was quenched with water (20 mL) and extracted with CH_2Cl_2 (20 mL × 3). The combined organic phases were dried over anhydrous Na_2SO_4 and concentrated under reduced pressure. The crude product was purified by silica gel column chromatography using petroleum ether/ethyl acetate (*v/v* = 20/1 to 10/1) as eluents to afford yellow oil **5** (0.36 g, 78%); ^1H NMR (600 MHz, $CDCl_3$, TMS) δ-0.19 (s, 9H, CH_3), 1.59–1.66 (m, 2H, $NCHCH_2$), 1.99 (s, 1H, N*H*), 2.73 (dd, *J* = 4.9, 11.6 Hz, 1H, NCH_2), 2.90 (dd, *J* = 2.1, 11.6 Hz, 1H, NCH_2), 3.69–3.71 (m, 1H, NC*H*), 4.27–4.38 (m, 3H, OC*H*, OCH_2), 5.13 (d, *J* = 11.0 Hz, 1H, $=CH_2$), 5.64 (d, *J* = 17.6 Hz, 1H, $=CH_2$), 6.61 (dd, *J* = 10.9, 17.6 Hz, 1H, =C*H*), 7.10–7.39 (m, 14H, Ar-*H*) ppm; ^{13}C NMR (151 MHz, $CDCl_3$): δ 2.1 (CH_3), 34.3 ($NCHCH_2$), 52.9 (NCH_2), 63.7 (N*C*H), 70.5, 79.2, 82.9 (OCH_2, O*C*H, O*C*$(CH_3)_3$), 113.7 ($=CH_2$), 126.2, 126.8, 126.9, 127.4, 127.5, 127.6, 127.8, 128.4, 136.5, 136.9, 138.1, 145.3, 146.6 (Ph, =*C*H) ppm.

Preparation of MNPs Fe_3O_4 and Fe_3O_4/PVP

$FeCl_3 \cdot 6H_2O$ (11.0 g, 40.7 mmol) and $FeCl_2 \cdot 4H_2O$ (4.0 g, 20.4 mmol) in water (50 mL) were mixed well at room temperature under argon. The reaction mixture was heated to 85 ℃ and then added aqueous ammonia (23%) dropwise to a pH of 8–9. After being aged at 85 ℃ for 4 h, the MNPs Fe_3O_4 were separated by magnetic decantation and washed with water to pH = 7. Subsequently, MNPs Fe_3O_4 (4.0 g) were well-dispersed in water (50 mL) and added aqueous polyvinylpyrrolidone (PVP) solution (10.0 mL, 25 g L^{-1}). After being stirred at room temperature for 12 h, the reaction mixture was added acetone (250 mL) and stirred for 10 min. The MNPs Fe_3O_4/PVP were obtained by magnetic decantation, washed with ethanol (50 mL × 2) and dried under vacuum at 55 ℃ for 24 h. Anal. Calcd for Fe_3O_4/PVP Found: C, 0.01; H, 0.23; N, 0.05.

Preparation of supported Jørgensen–Hayashi catalysts $Fe_3O_4@SiO_2$/ProTMS and $Fe_3O_4/PVP@SiO_2$/ProTMS

A mixture of 3-mercaptotrimethoxysilane (MPTMS, 0.25 mL, 1.14 mmol), AIBN (41.0 mg, 0.25 mmol) and **5** (0.23 g, 0.5 mmol) in 15 mL of $CHCl_3$ was stirred at 80 ℃ for 12 h under a N_2 atmosphere and the solvent was removed under reduced pressure. The residues containing MPTMS and ProTMS were added slowly to ethanol solution containing Fe_3O_4 or Fe_3O_4/PVP (25 mL, 125.0 mg) pretreated with aqueous ammonia (0.75 mL, 23%) and tetraethyl orthosilicate (0.13 mL, TEOS) for 2 h. After the resulting mixture was stirred at room temperature for 24 h, the pale yellow MNPs-supported Jørgensen–Hayashi $Fe_3O_4@SiO_2$/ProTMS (0.46 g) and $Fe_3O_4/PVP@SiO_2$/ProTMS (0.57 g) catalysts were separated magnetically, washed with $CHCl_3$ (25 mL × 3), ethanol (25 mL × 3) and dried under vacuum for 4 h. Anal. Calcd for $Fe_3O_4@SiO_2$/ProTMS Found: C, 31.51; H, 4.10; N, 1.02; S, 6.15 and $Fe_3O_4/PVP@SiO_2$/ProTMS Found: C, 31.56; H, 3.22; N, 0.90; S, 5.42.

General procedure for the Michael reaction

A reaction mixture of (*E*)-nitrostyrene (40.0 mg, 0.27 mmol), $Fe_3O_4/PVP@SiO_2$/ProTMS (30.0 mg, 7 mol%) and $CHCl_3$ (2.0 mL) was stirred at 0 ℃ for 10 min, added propanal (94.0 mg, 1.62 mmol) by syringe and monitored by TLC until completion. The catalyst was separated using an external magnetic field, washed with $CHCl_3$ (2.0 mL × 3) and reused directly for the next catalytic cycle. The combined organic layers were concentrated and purified by silica gel column chromatography using petroleum ether/ethyl acetate (*v/v* = 5/1) as eluents to afford the Michael adduct. The diastereoselectivities (*syn/anti*) and enantioselectivities (% ee) of products were determined by ^1H NMR and HPLC on a chiral stationary phase (Daicel Chiralpak OD-H, AD-H, AS-H or OJ-H, 4.6 mm × 25 cm column, see ESI†), respectively.

Results and discussion

Preparation of MNPs-supported organocatalyst

As described in Scheme 2, Jørgensen–Hayashi catalyst **5** could be synthesized using Boc-L-hydroxyproline as starting material with the moderate to good yields in each step (77–95%).[14] The TEM image showed that the spherical MNPs of Fe_3O_4 with the 20–30 nm dimeters could be generated at a pH of 8–9 by simple co-precipitation of $FeCl_3$ and $FeCl_2$ with molar ratio of 2 in the presence of aqueous ammonia (23%). After being modified for 12 h at room temperature in aqueous PVP solution, TEM image revealed that MNPs Fe_3O_4/PVP had no significant change in the surface morphology and particle diameter. According to the

the content of nitrogen (0.05%) detected by elemental analysis, the loading of PVP onto the backbone of Fe_3O_4 was calculated to be very low (about 0.4%).

As described in Scheme 1, the Jørgensen–Hayashi catalyst **5** attached to ProTMS could be immobilized by one-pot to prepare the supported organocatalysts Fe_3O_4@SiO_2/ProTMS and Fe_3O_4/PVP@SiO_2/ProTMS through the radical addition of sulfydryl (-SH) to C=C double bond in **5** and subsequent surface-modification taking advantage of the hydrolysis of $Si(OCH_3)_3$ on the surface of MNPs Fe_3O_4 and Fe_3O_4/PVP. Based to the nitrogen contents by elemental analysis (1.02% and 0.90%), the loading capacities of Jørgensen–Hayashi catalyst **5** in Fe_3O_4@SiO_2/ProTMS and Fe_3O_4/PVP@SiO_2/ProTMS were calculated to be 0.73 mmol g^{-1} and 0.64 mmol g^{-1}, respectively. Moreover, the loadings of MPTMS onto Fe_3O_4@SiO_2/ProTMS and Fe_3O_4/PVP@SiO_2/ProTMS were also determined by elemental analysis of sulphur (6.15% and 5.42%) to be 1.92 mmol g^{-1} and 1.69 mmol g^{-1}. Owing to the partial radical addition of sulfydryl (-SH) to C=C double bond in **5**, the free MPTMS were found to be 1.19 mmol g^{-1} and 1.05 mmol g^{-1}. Based on the loaded MPTMS and ProTMS, it was found that Fe_3O_4@SiO_2/ProTMS and Fe_3O_4/PVP@SiO_2/ProTMS possessed the same molar ratio (1.6/1) of free MPTMS to ProTMS. Furthermore, the superparamagnetic behavior of Fe_3O_4@SiO_2/ProTMS (21.5 emu g^{-1}) and Fe_3O_4/PVP@SiO_2/ProTMS (10.4 emu g^{-1}) at 298 K was evidenced by the zero coercivity and resonance of each magnetization loop in the magnetization curves (Fig.1).

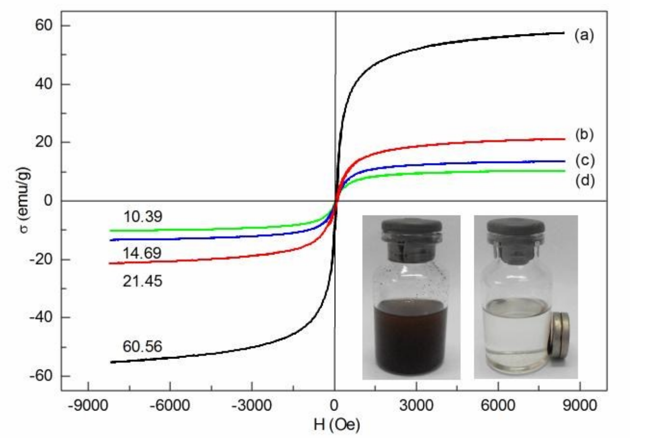

Fig.1 Magnetization curves for Fe_3O_4/PVP (a), Fe_3O_4@SiO_2/ProTMS (b), 10th-recycled Fe_3O_4/PVP@SiO_2/ProTMS (c) and Fe_3O_4/PVP@SiO_2/ProTMS (d).

The role of polyvinylpyrrolidone (PVP)

Poly(vinylpyrrolidone) (PVP, K29–32), amphiphilic and nonionic polymer, was widely used in science and technology, and could be adsorbed onto a broad range of different materials as stabilizing agent.[15] Herein, we endeavoured to elucidate where PVP was adsorbed onto the backbone of MNPs Fe_3O_4 and what changes in chemical and physical properties were resulted from PVP.

The covalent attachment of Jørgensen–Hayashi catalyst **5** to the backbone of Fe_3O_4 MNPs is clearly corroborated by FT-IR spectroscopy (Fig. 2), which confirmed by (1) the asymmetrical, symmetrical stretching vibration and flexural vibration of Si-O-Si at 1067, 807 and 459 cm^{-1},[16] (2) the stretching vibrations of C-S and Si-C bonds at 1249 and 702 cm^{-1},[17] (3) the various C–H stretching vibrations and characteristic phenyl ring at 3056, 3025, 2930 cm^{-1} and in the 1632–1448 cm^{-1} range, respectively. After being modified by PVP (0.4%), there was no significant difference in IR spectra between Fe_3O_4/PVP and bare Fe_3O_4. Furthermore, all Fe_3O_4/PVP@SiO_2/ProTMS and Fe_3O_4@SiO_2/ProTMS had a strong stretching vibration of C-O bond at 1134 cm^{-1}, which implied that a large amount of $–SiOCH_3$ moieties existed on the surface of Fe_3O_4/PVP@SiO_2/ProTMS and Fe_3O_4@SiO_2/ProTMS.

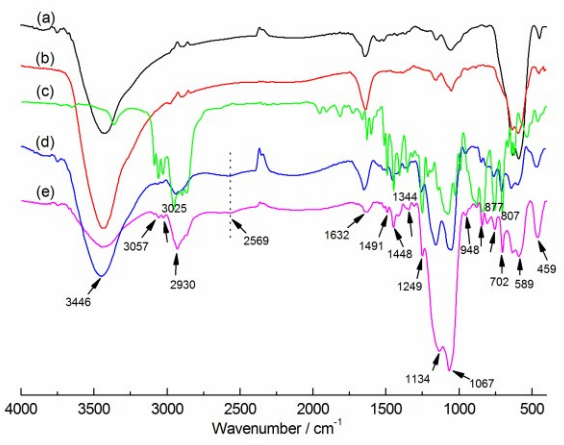

Fig.2 IR spectra of Fe_3O_4 MNPs (a), Fe_3O_4/PVP MNPs (b), Jørgensen–Hayashi catalyst 5 (c), Fe_3O_4/PVP@SiO_2/ProTMS (d) and Fe_3O_4@SiO_2/ProTMS (e)

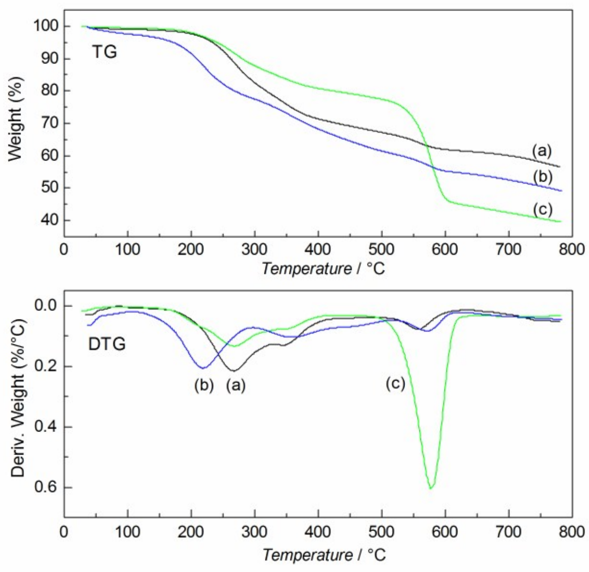

Fig.3 Thermogravimetric curves of Fe_3O_4@SiO_2/ProTMS (a), 10th-recycled Fe_3O_4/PVP@SiO_2/ProTMS (b) and Fe_3O_4/PVP@SiO_2/ProTMS (c).

The effect of PVP on the hydrolysis degree of $-Si(OCH_3)_3$ attached to ProTMS and MPTMS onto MNPs Fe_3O_4/PVP and Fe_3O_4 could be further monitored by TGA. From the TG and DTG curves (Fig. 3), the thermal decomposition of organic moieties in Fe_3O_4/PVP@SiO_2/ProTMS occurred in two distinct steps: the first one in the temperature 200–500 ℃ range and the second one in the 500–600 ℃ range, accompanied by a continuous endothermic peak (see ESI†). It is noteworthy that Fe_3O_4/PVP@SiO_2/ProTMS exhibited the 15.2% higher weight loss than Fe_3O_4@SiO_2/ProTMS in the temperature range of 200–600 ℃, although Fe_3O_4/PVP@SiO_2/ProTMS contained a lower amount of Jørgensen–Hayashi catalyst **5**. Another phenomenon was that a sharp weight loss of Fe_3O_4/PVP@SiO_2/ProTMS (30.01%) was newly emerged in the 500–600 ℃ range (Fig. 3c). Based on the two points mentioned above, it was demonstrated that the hydrolysis efficiency of -Si(OCH_3)$_3$ decreased upon the attachment of ProTMS and MPTMS onto Fe_3O_4/PVP, and resulted in the increased $SiOCH_3$ moiety due to the package of PVP, which was in accord with the stronger C-O stretching vibration at 1134 cm^{-1} in IR spectra of Fe_3O_4/PVP@SiO_2/ProTMS and verified by the weakened C-O stretching vibration of 10th-recycled Fe_3O_4/PVP@SiO_2/ProTMS. Furthermore, besides the same typical peaks of Fe_3O_4 at 30.3°, 35.6°, 43.3°, 53.8°, 57.4° and 63.0° in the XRD pattern, Fe_3O_4@SiO_2/ProTMS and Fe_3O_4/PVP@SiO_2/ProTMS also displayed the difference in the typical peak of SiO_2 in the 16–25 ° range (Fig. 4a, b), which was closely evidenced to the hydrolysis degree of -Si(OCH_3)$_3$.

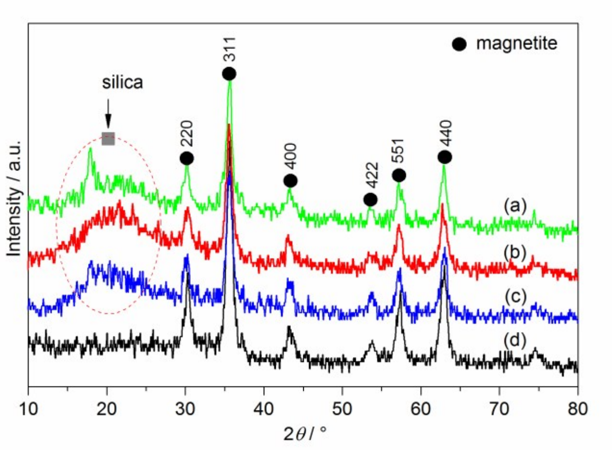

Fig.4 Powder X-ray diffraction patterns of Fe_3O_4/PVP@SiO_2/ProTMS (a), Fe_3O_4@SiO_2/ProTMS (b), 10th-recycled Fe_3O_4/PVP@SiO_2/ProTMS (c) and Fe_3O_4 MNPs (d).

The presence of PVP not only altered the chemical composition but also affected the morphology of MNPs-supported catalyst. The grafting of Jørgensen–Hayashi catalyst **5** onto MNPs Fe_3O_4 and Fe_3O_4/PVP led to a serious agglomeration due to the coated SiO_2 generated from the hydrolysis of -Si(OCH_3)$_3$ moiety. However, seen from the SEM images, Fe_3O_4/PVP@SiO_2/ProTMS exhibited the smaller even-textured and granular particles with the diameters ranging from 0.2 to 0.3 um (Fig. 5f), compared with irregular Fe_3O_4@SiO_2/ProTMS (Fig. 5b). The further investigation by the TEM image showed the densely agminated Fe_3O_4@SiO_2/ProTMS (Fig. 5d) and nano-structured Fe_3O_4/PVP@SiO_2/ProTMS (Fig. 5h) in an accumulative state upon being coated with SiO_2 shell, respectively due to the profound and weakened hydrolysis of -Si(OCH_3)$_3$ in the absence or presence of PVP.

The nitrogen adsorption–desorption isotherm plots of all samples, obtained at 77 K, were shown in ESI†. After being stirred at room temperature polyvinylpyrrolidone (PVP) solution

View Article Online
DOI: 10.1039/C6RA01050E

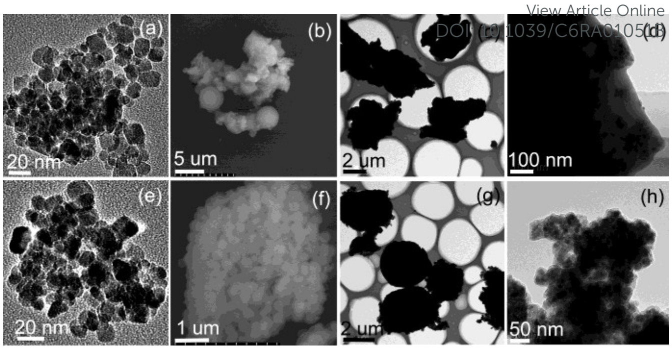

Fig.5 The surface morphologies for TEM of MNPs Fe_3O_4 (a), SEM of Fe_3O_4@SiO_2/ProTMS (b), TEM of Fe_3O_4@SiO_2/ProTMS (c, d), TEM of MNPs Fe_3O_4/PVP (e), SEM of Fe_3O_4/PVP@SiO_2/ProTMS (f), TEM of of Fe_3O_4/PVP@SiO_2/ProTMS (g, h).

(10.0 mL, 25 g L^{-1}) for 12 h, it was found that MNPs Fe_3O_4/PVP possessed the higher BET-specific surface area (65.8 m^2 g^{-1}), average pore diameter (11.7 nm) and pore volume (0.39 cc g^{-1}) than bare Fe_3O_4 (7.9 m^2 g^{-1}, 5.2 nm and 0.021cc g^{-1}). Especially, Fe_3O_4/PVP had five characteristic cavities centered at 0.9, 1.4, 2.1, 3.4 and 6.6 nm, accompanied by some additional pores in the different sizes with the nitrogen desorption (Dv) (< 1.0 × 10^{-3} mL $Å^{-1}$ g^{-1}) (Fig. 6c), whereas bare MNPs Fe_3O_4 displayed a broad pore size distribution (Fig. 6a). Interestingly, except for these five characteristic cavities, all the other pores in Fe_3O_4/PVP disappeared upon the immobilization of ProTMS and MPTMS through the hydrolysis of -Si(OCH_3)$_3$, which indicated that Jørgensen–Hayashi catalyst **5** was entrapped inside these disappeared pores. To our delight, the remained four characteristic pores of Fe_3O_4/PVP@SiO_2/ProTMS with the high Dv values (> 1.0 × 10^{-3} mL $Å^{-1}$ g^{-1}) provided the crucial channels for reactants to access catalytic sites in catalytic process. Unfortunately, Fe_3O_4@SiO_2/ProTMS exhibited the non-uniform pore size distribution in the 1–10 nm range without the modification of PVP.

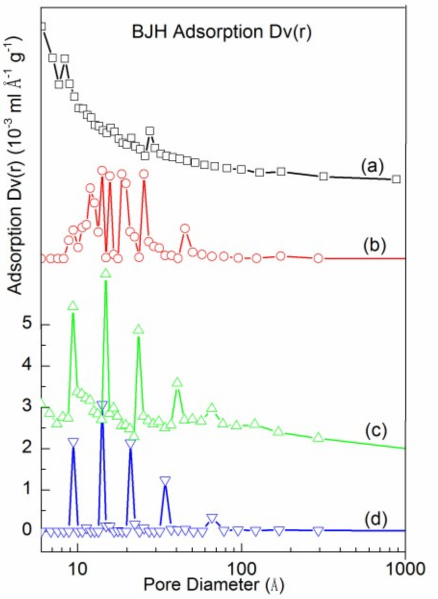

Fig.6 Pore size distributions (PSDs) of Fe_3O_4 (a), Fe_3O_4@SiO_2/ProTMS (b), Fe_3O_4/PVP (c) and Fe_3O_4/PVP@SiO_2/ProTMS (d).

View Article Online
DOI: 10.1039/C6RA01051B

Asymmetric Michael addition

To evaluate influence of PVP on the catalytic performance and reusability of $Fe_3O_4@SiO_2$/ProTMS and Fe_3O_4/PVP@SiO_2/ProTMS, the asymmetric Michael addition of propanal to *trans*-*β*-nitrostyrene was selected as a model reaction.

In the Michael addition of propanal to *trans*-*β*-nitrostyrene, the corresponding *syn*-adducts, whose absolute stereochemistry was determined to be 2*R*, 3*S*-configurations by comparing its optical rotation and HPLC spectra with literature values,[18] were obtained as major steroisomers in the high yields and excellent enantioselectivities (Table 1). To the best of our knowledge, it was found that Fe_3O_4/PVP@SiO_2/ProTMS appeared as the most efficient MNPs–supported Jørgensen–Hayashi catalyst to date in terms of catalytic activity, steroselectivity and reusability among the ever-reported Michael additions.[11–13] Meanwhile, Fe_3O_4 /PVP@SiO_2/ProTMS (99%, *syn/anti* = 92/8, 98% ee) presented the superior catalytic performances to $Fe_3O_4@SiO_2$/ ProTMS (89%, *syn/ anti* = 89/11 and 95% ee) (entry 18), which might be rationalized in terms of catalytic accessibility and steric confinement owing the above-mentioned structural texture and morphology resulted from the vital function of PVP. In the following catalytic reactions, Fe_3O_4/PVP@SiO_2/ProTMS was chosen for the further optimization of experimental conditions.

Table 1 Screening of reaction conditions of Fe_3O_4/PVP@SiO_2/ProTMS for the Michael addition of propanal to *trans*-*β*-nitrostyrene [a]

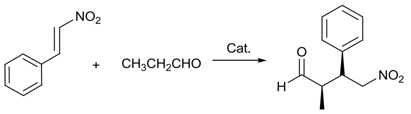

Entry	Catalyst (mg/mol%)	Addictive	Solvent	*T*/h (°C / h)	Yield (%)[b]	*Syn/anti*[c]	ee (%)[d]
1	30/7	-	$CHCl_3$	0/17	99	89/11	97
2	30/7	TFA	$CHCl_3$	0/8	trace	n.d.	n.d.
3	30/7	$PhCO_2H$	$CHCl_3$	0/12	93	92/8	97
4	30/7	2-$FPhCO_2H$	$CHCl_3$	0/12	95	90/10	97
5	30/7	3-NO_2PhCO_2H	$CHCl_3$	0/8	99	96/4	98
6	30/7	3-NO_2PhCO_2H[e]	$CHCl_3$	0/24	93	93/7	97
7	30/7	3-NO_2PhCO_2H	$C_6H_5CH_3$	0/8	87	88/12	95
8	30/7	3-NO_2PhCO_2H	CH_2Cl_2	0/8	94	90/10	96
9	30/7	3-NO_2PhCO_2H	EtOH	0/8	trace	n.d.	n.d.
10	60/14	-	$CHCl_3$	0/8	98	91/9	97
11	60/14	3-NO_2PhCO_2H	$CHCl_3$	0/4	98	91/9	98
12	15/3.5	-	$CHCl_3$	0/32	76	92/8	97
13	15/3.5	3-NO_2PhCO_2H	$CHCl_3$	0/22	96	89/11	98
14	30/7	3-NO_2PhCO_2H	$CHCl_3$	20/5	99	87/13	96
15	30/7	3-NO_2PhCO_2H	$CHCl_3$	10/7	99	90/10	97
16	30/7	3-NO_2PhCO_2H	$CHCl_3$	-10/20	86	96/4	98
17	30/7	3-NO_2PhCO_2H	$CHCl_3$	-20/32	82	98/2	98
18[f]	26/7	3-NO_2PhCO_2H	$CHCl_3$	0/8	89	93/7	97

[a] Reaction conditions: *trans*-*β*-Nitrostyrene (40 mg, 0.27 mmol), propanal (94 mg, 1.62 mmol), additive (10 mol%), solvent (2.0 mL). [b] Isolated yield. [c] Determined by ^1H NMR. [d] Determined by chrial HPLC. [e] 20 mol% of additive. [f] $Fe_3O_4@SiO_2$/ProTMS used.

Firstly, it was found that the acid strengths of brøsted acids such as TFA (pK_a = 0.23), 3-$NO_2C_6H_4CO_2H$ (pK_a = 2.45), 2-$FC_6H_4CO_2H$ (pK_a = 3.27) and $C_6H_4CO_2H$ (pK_a = 4.21) had a

Table 2 Asymmetric Michael addition of propanal to various nitroalkenes catalyzed by Fe_3O_4/PVP@SiO_2/ProTMS [a]

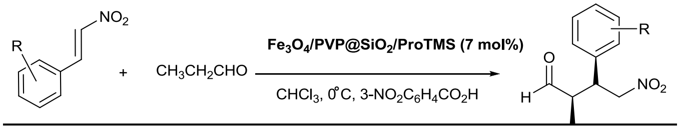

Entry	t (h)	Product	Yield (%)[b]	*Syn/anti*[c]	% ee[d]
1	8	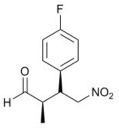	98	88/12	97
2	7	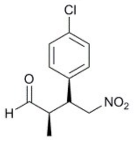	99	87/13	97
3	9	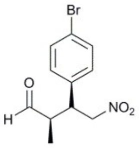	95	86/14	96
4	24	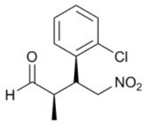	98	88/12	96
5	48	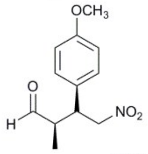	99	92/8	97
6	12	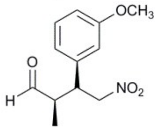	97	89/11	96
7	48	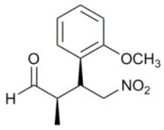	93	92/8	96
8	12	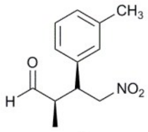	98	89/11	96
9	48	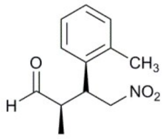	95	90/10	97
10	11	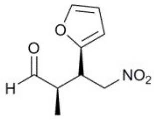	98	81/19	95

View Article Online
DOI: 10.1039/C6RA01051B

11	34	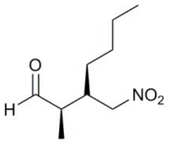	97	86/14	97
12	8	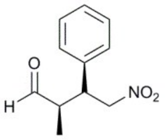	>99	96/4	98

[a] Reaction conditions: Nitrolefin (40 mg, 0.27 mmol), propanal (94 mg, 1.62 mmol), 3-$NO_2C_6H_4CO_2H$ (10 mol%), $CHCl_3$ (2.0 mL), 0 ℃. [b] Isolated yield. [c] Determined by ^{1}H NMR. [d] Determined by chrial HPLC.

great effect on catalytic performances (entries 2-6). Disappointedly, TFA with the stronger acid strength only afforded a trace of Michael adduct (entry 2). Fortunately, the other weak brøsted acids could effectively improve catalytic rate and stereoselectivity. Among them, 3-$NO_2C_6H_4CO_2H$ (10 mol%) was proved to be the best effective co-catalyst with the excellent performances (99%, *syn/anti* = 96/4, 98% ee, entry 5). It was worthwhile to note that Fe_3O_4/PVP@SiO_2/ProTMS gave the less catalytic performances (93%, *syn/anti* = 93/7, 97% ee, entry 6) after 24 h upon doubling the dosage of 3-$NO_2C_6H_5CO_2H$. Next, the effects of temperature, solvent and used amount of catalyst on catalytic performance were further screened out in detail. Our attempts to further reduce catalyst loading led to the decreased yield and stereoselectivity (entries 12, 13), and ethanol as a solvent resulted in no activity (entry 9). Furthermore, although the decrease in temperature to -20 ℃ led to the product with the higher steroselectivity (*syn/anti* = 98/2, 98% ee, entry 17), it took place at a considerably lower rate, requiring up to 32 h for the achievement of 82% yield.

The optimized protocol was expanded to a wide variety of *trans*-*β*-nitrostyrenes bearing electron-donating (-CH_3, OCH_3) and electron-withdrawing (-X) substituents at the *o*, *m*, *p*-positions. From Table 2, all *trans*-*β*-nitrostyrenes bearing electron-donating and electron-withdrawing substituents afforded the excellent catalytic performances at the same level (93–99%, *syn/anti* = 86–92:14–8, 96–98% ee, entries 1–9). It was worthwhile to note that the nitrostyrenes with *o*, *p*-OCH_3 and *o*-CH_3 electron-donating (entries 5, 7 and 9) and *o*-Cl electron-withdrawing substituent (entry 4) required respective 48 h and 24 h to achieve the 93–99% yields resulted from the electron-donating effect and vicinal hidrance of the substituents. A nitroalkene bearing a heterocyclic 2-furyl substituent also afforded a high 98% yield and 95% ee but gave a moderate diasteroselectivity (*syn/anti* = 81/19) (entry 10). Additionally, the Michael addition of propanal to aliphatic nitroalkene gave the good catalytic performances (97%, 97% *ee*, 86:14 *dr*) but needed a prolonged reaction period (34 h, entry 11).

Reusability of MNPs-supported catalyst

One of the main advantages associated with the supporting of a catalyst onto MNPs is the facile separation of a catalyst from reaction mixture with an external magnet. When the reaction was completed, an external magnet was put nearby the reaction flask to concentrate Fe_3O_4/PVP@SiO_2/ProTMS, and the solution could be easily decanted. The recovered catalyst was directly reused for the next run after being washed with $CHCl_3$ (2.0 mL × 3).

Fig. 7 showed the comparative reusabilities of Fe_3O_4/PVP@SiO_2/ProTMS and Fe_3O_4@SiO_2/ProTMS including the yields and steroselectivities. From Fig.6, Fe_3O_4/PVP@SiO_2/ProTMS displayed a better reusability than Fe_3O_4@SiO_2/ProTMS. Unfortunately, the decreasing yields and diasteroselectivity catalyzed by Fe_3O_4@SiO_2/ProTMS after the second run like the ever-reported Jørgensen–Hayashi catalysts using MNPs as a support.[11–13] On the contrary, the yields catalyzed by Fe_3O_4/PVP@SiO_2/ProTMS remained at the very high level (>94%) in the first five cycles. Even in 10th run, the 77% yield could be achieved after prolonging the reaction time to 48 h. More excitedly, the constant excellent stereoselectivity (98% ee and 96/4 *dr*) could be maintained in the ten consecutive cycles. To the best of our knowledge, Fe_3O_4/PVP@ProTMS exhibited the most effective reusability among the reported MNPs-supported Jørgensen–Hayashi catalysts.

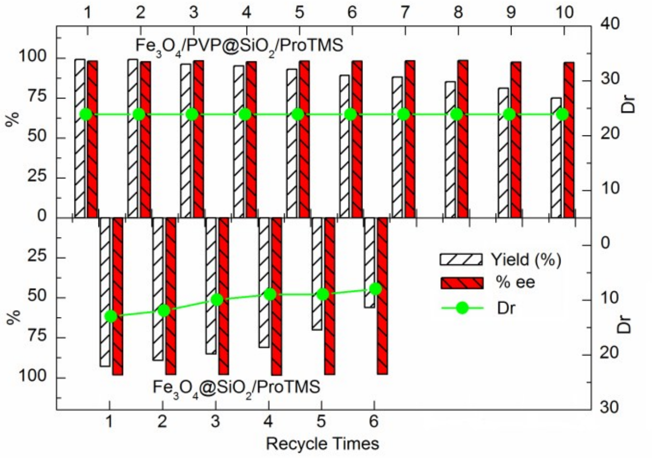

Fig. 7 The comparative reusability of Fe_3O_4@SiO_2/ProTMS and Fe_3O_4/PVP@SiO_2/ProTMS under the optimized reaction conditions.

To understand the reason for the decreased yield, the structural change of the 10th-recycled Fe_3O_4/PVP@SiO_2/ProTMS was monitored by TEM, TGA, elemental analysis and N_2 adsorption–desorption isotherm. Above all, the increased carbon, hydrogen and nitrogen contents, especially the doubled nitrogen content (0.90%→1.76%) stemmed from nitrogenous compounds such as nitroalkene, elucidated that the reactants and products were adsorbed on the porous backbone of the catalyst, which also verified by the decreased average pore size and pore volume from 15.7 nm and 0.031 cc g^{-1} to 2.5 nm and 0.021 cc g^{-1} respectively. Moreover, the structural change of SiO_2 attached on the core of Fe_3O_4/PVP was elucidated by XRD and TGA, in which a wide and round XRD peak of SiO_2 in the range of 16–25 ° (Fig. 3b) and a disappeared weight loss in the 500–600 ℃ range demonstrated the further hydrolysis of -$SiOCH_3$. Meanwhile, it was found that the 10th-recycled Fe_3O_4/PVP@SiO_2/ProTMS maintained its original magnetic property (Fig. 1b) and no agglomeration was observed by TEM (Fig. S10, ESI†). In conclusion, it was speculated that the adsorbed impurities and further hydrolysis of -$SiOCH_3$ resulted in the structural changes such as pore volume and pore size distribution and was ultimately responsible for the decreased catalytic activity of Fe_3O_4/PVP@SiO_2/ProTMS.

Conclusions

In summary, we had immobilized the homogeneous Jørgensen–Hayashi catalyst of (S)-diphenylprolinoltrimethylsilyl ether onto the backbone of Fe_3O_4/PVP *via* facile one-pot surface-modification, and successfully applied the MNPs Fe_3O_4-supported catalyst Fe_3O_4 /PVP@SiO_2/ProTMS in the asymmetric Michael addition of propanal to various nitroalkenes with excellent catalytic performances. Due to the adsorbed poly (vinylpyrrolidone) (PVP), Fe_3O_4/PVP@SiO_2/ProTMS had a great change in chemical composition, surface morphology and pore structure related to the hydrolysis degree of -$Si(OCH_3)_3$, which provided a suitable micro-environment to achieve the good reusability with the high yields and unchangeable excellent steroselectivities including *syn/ anti* and % ee for the first time.

Acknowledgements

We are grateful to the Fundamental Research Funds for the Central Universities (XDJK2015D028) and the National Science Foundation of China (621362005).

Notes and references

1 a) M. Marigo, T. C. Wabnitz, D. Fielenbach and K. A. Jϕrgensen, *Angew. Chem. Int. Ed*., 2005, **44**, 794-797; b) J. Franzén, M. Marigo, D. Fielenbach, T. C. Wabnitz, A. Kjærsgaard and K. A. Jϕrgensen, *J. Am. Chem. Soc*., 2005, **127**, 18296–18304; c) Y. Hayashi, H. Gotoh, T. Hayashi, M. Shoji, *Angew. Chem. Int. Ed*., 2005, **44**, 4212– 4215.
2 S. Mukherjee, J. W. Yang, S. Hoffmann and B. List, *Chem. Rev*., 2007, **107**, 5471–5569.
3 A. Erkkilä, I. Majander and P. M. Pihko, *Chem. Rev*., 2007, **107**, 5416– 5470.
4 S. Meninno and A. Lattanzi, *Chem. Commun.*, 2013, **49**, 3821–3832.
5 a) C. M. R. Volla, I. Atodiresei and M. Rueping, *Chem. Rev*., 2014, **114**, 2390–2431; b) A. Z. Halimehjani, I. N. N. Namboothiri and S. E. Hooshmand, *RSC Adv*., 2014, **4**, 51794–51829; c) Hélène Pellissier,*Tetrahedron*, 2013, **69**, 7171–7210.
6 a) X. J. Li, B. L. Yang, X. B. Jia, M. Q. Chen and Z. G. Hu, *RSC Adv*., 2015, **5**, 89149-89156; b) S. Wang, P. W. Liu, W. J. Wang, Z. G. Zhang and B. G. Li, *Catal. Sci. Technol*., 2015, **7**, 3798–3805; c) C. Schafer, S. C. Mhadgut, N. Kugyela, M. Torok and B. Torok, *Catal. Sci. Technol*., 2015, **7**, 716–723; d) A. Lu, T, P, Smart, T. H. Epps, D. A. Longbottom and R. K. O'Reilly, *Macromolecules*, 2011, **44**, 7233–7241; e) K. Akagawa, S. Sakamoto, K. Kudo, *Synlett*., 2011, **6**, 817–820; f) E. Alza and M. A. Pericàs, *Adv. Synth. Catal*., 2009, **351**, 3051– 3056.
7 a) A. A. Elmekawy, J. B. Sweeney, D. R. Brown, *Catal. Sci. Technol*., 2015, **7**, 716–723; b) C. L. Wu, X. Q. Long, X. K. Fu, G. W. Wang and Z. A. Mirza, *RSC Adv.*, 2015, **5**, 3168–3176; c) M. Angeloni, O. Piermatti, F. Pizzo and L. Vaccaro, *Eur. J. Org. Chem.*, 2014, **8**, 1716–1726; d) S. Calogero, D. Lanari, M. Orru, O. Piermatti, F. Pizzo and L. Vaccaro, *J. Catal*., 2011, **282**, 112–119; e) W. Zheng, C. F. Lu, G. C. Yang, Z. X. Chen and J. Q. Nie, *Catal. Commun*., 2015, **62**, 34–38.
8 a) Y. Kong, R. Tan, L. L. Zhao and D. H. Yin, *Green Chem*., 2013, **15**, 2422–2433; b) X. Zhang, W. S. Zhao, C. K. Qu, L. L. Yang and Y. C. Cui, *Tetrahedron-Asymmetry*, 2012, **23**, 468–473.
9 R. Tan, C. Y. Li, J. Q. Luo, Y. Kong, W. G. Zheng and D. H. Yin, *J. Catal.*, 2013, **298**, 138–147.
10 a) R. B. N. Baig, M. N. Nadagouda and R. S. Varma, *Coord. Chem. Rev*., 2015, **287**, 137–156; b) R. Dalpozzo, *Green Chem*., 2015, **17**, 3671–3686; c) J. W. Wan, L. ding, T. Wu, X. B. Ma and Q. Tang, *RSC Adv*., 2014, **4**, 38323–38333.
11 B. G. Wang, B. C. Ma, Q. Wang and W. Wang, *Adv. Synth. Catal.*, 2010, **352**, 2923–2928
12 P. Riente, C. Mendoza and M. A. Pericás, *J. Mater. Chem*., 2011, **21**, 7350–7355.
13 M. Keller, A. Perrier, R. Linhardt, L. Travers, S. Wittmann, A. M. Caminade, J. P. Majoral, O. Reiser and A. Oualia, *Adv. Synth. Catal*., 2013, **355**, 1748–1754.
14 A. B. Xia, C. Z., Y. P. Zhang, Y. J. Guo, X. L. Zhang, Z. B. Li and D. Q. Xu, *Org. Biomol. Chem*., 2015, **13**, 9593–9599.
15 a)T. J. Yoon, J. S. Kim, B. G. Kim, K. N. Yu, M. H. Cho and J. K. Lee, *Angew. Chem. Int. Ed.*, 2005, 44, 1068–1071; b) M. Shokouhimehr, Y. Piao, J. Kim, Y. Jang and T. Hyeon, *Angew. Chem. Int. Ed*., 2007, 46, 7039–7043; c) X. X. Zheng, S. Z. Luo, L. Zhang and J. P. Cheng, *Green Chem*., 2009, **11**, 455–458.
16 a) A. Khalafi-Nezhad, E. S. Shahidzadeh, S. Sarikhani and F. Panahi, *J. Mol. Catal. A: Chem.*, 2013, **379**, 1-8; b) A. Khalafi-Nezhad and F. Panahi, *Green Chem*., 2011, **13**, 2408-2415; c) D. D. Feng, J. H. Xu, J. W. Wan, B. Xie and X. B. Ma, *Catal. Sci. Technol*., 2015, **5**, 2141–2148
17 L. L. Lou, H. L. Du, Y. B. Shen, K. Yu, W. J. Yu, Q. Chen and S. X. Liu, Microporous Mesoporous Mater., 2014, **187**, 94–99; Y. Du, D. D. Feng, J. W. Wan and X. B. Ma, *Appl. Catal. A: General*, 2014, *479*, 49–58; W. Wang, X. B. Ma, J. W. Wan, J. Cao and Q. Tang, *Dalton Trans*., 2012, **41**, 5715–5726.
18 a) Y. Hayashi, H. Gotoh, T. Hayashi and M. Shoji, *Angew. Chem. Int. Ed.*, 2005, 44, 4212; b) Z. L. Zheng, B. L. Perkins and B. Ni, *J. Am. Chem. Soc*., 2010, **132**, 50–51.

View Article Online
DOI: 10.1039/C6RA01051B

Table of contents entry

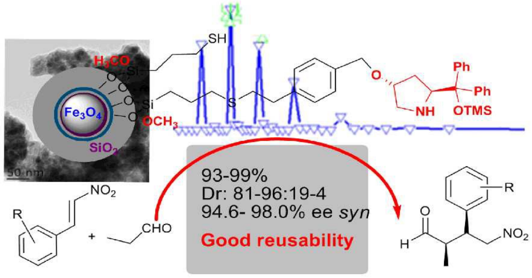

PVP-modified MNPs Fe_3O_4-supported Jøgensen-Hayashi catalyst provided suitable microenvironments to achieve the good reusability with the high yields and unchangeable excellent steroselectivities in the asymmetric Michael addition of propanal to nitroalkenes.